REVIEW

Electrode Materials for Rechargeable Sodium-Ion Batteries: Potential Alternatives to Current Lithium-Ion Batteries

Sung-Wook Kim, Dong-Hwa Seo, Xiaohua Ma, Gerbrand Ceder, and Kisuk Kang**

Lithium (Li)-ion batteries (LIB) have governed the current worldwide rechargeable battery market due to their outstanding energy and power capability. In particular, the LIB's role in enabling electric vehicles (EVs) has been highlighted to replace the current oil-driven vehicles in order to reduce the usage of oil resources and generation of CO_2 gases. Unlike Li, sodium is one of the more abundant elements on Earth and exhibits similar chemical properties to Li, indicating that Na chemistry could be applied to a similar battery system. In the 1970s-80s, both Na-ion and Li-ion electrodes were investigated, but the higher energy density of Li-ion cells made them more applicable to small, portable electronic devices, and research efforts for rechargeable batteries have been mainly concentrated on LIB since then. Recently, research interest in Na-ion batteries (NIB) has been resurrected, driven by new applications with requirements different from those in portable electronics, and to address the concern on Li abundance. In this article, both negative and positive electrode materials in NIB are briefly reviewed. While the voltage is generally lower and the volume change upon Na removal or insertion is larger for Na-intercalation electrodes, compared to their Li equivalents, the power capability can vary depending on the crystal structures. It is concluded that cost-effective NIB can partially replace LIB, but requires further investigation and improvement.

1. Introduction

Since Sony announced the first version of commercialized lithium (Li)-ion battery (LIB) in 1991, LIB has rapidly penetrated into everyday life.[1–4] Compared to other types of rechargeable battery systems, LIB exhibits superb performances in terms of energy density.[4–8] Small and light battery packages have enabled the worldwide uses of portable electronics (e.g., laptop, cellular phone, MP3 players) for the past decades. In recent years, driven by the increased desire for 'green' technologies, the use of LIB has expanded from portable electronics to large scale applications, in particular, electric vehicles (EVs).[4,5]

There has also been recent concern that the amount of the Li resources that are buried in the earth would not be sufficient to satisfy the increased demands on LIB.[9] While there is ample evidence that this is no cause for immediate concern,[10] very large market share of electric vehicles can put a strain on Li production capability. According to a Japanese report published in 2010,[9] about 7.9 million tons of metallic Li will be required when 50% of the oil-driven cars in the world are replaced by XEVs (including hybrid EVs (HEVs) and plug-in HEVs (PHEVs)) as shown in **Figure 1**. Although the prediction in reference [9] involves significant assumption and, for example, overestimates the amount of Li required per kWh of stored energy, it indicates that in the long term the cost of Li may increase as demand increases. Therefore, making provision beyond the LIB is important and alternatives with different chemistries have to be suggested.[11–14]

Sodium (Na) is located below Li in the periodic table and they share similar chemical properties in many aspects. The fundamental principles of the NIB and LIB are identical; the chemical potential difference of the alkali-ion (Li or Na) between two electrodes (anode and cathode) creates a voltage on the cell. In charge and discharge the alkali ions shuttle back and forth between the two electrodes. There are several reasons to investigate Na-ion batteries. As battery applications extend to large-scale storage such as electric buses or stationary storage connected to renewable energy production, high energy density becomes less critical. Moreover, the abundance and low cost of Na in the earth can become an advantage when a large amount of alkali is demanded for large-scale applications, though at this point, the cost of Li is not a large contribution to the cost of LIBs. But most importantly, there may be significant unexplored opportunity in Na-based systems, Na-intercalation chemistry has been explored considerably less than Li-intercalation, and early evidence seems to indicate that structures that do not function well as Li-intercalation compounds may work well with Na.[15] Hence, there may be opportunity to find novel electrode materials for NIB.

Important battery performance characteristics such as specific capacity and operation voltage are mainly determined by the

Dr. S.-W. Kim, Dr. D.-H. Seo, Prof. K. Kang
Department of Materials Science and Engineering
Seoul National University
Seoul 151-742, Republic of Korea
E-mail: matlgen1@snu.ac.kr
Dr. X. Ma, Prof. G. Ceder
Department of Materials Science and Engineering
Massachusetts Institute of Technology
Cambridge, MA 20139-4307, United States of America
E-mail: gceder@mit.edu

DOI: 10.1002/aenm.201200026

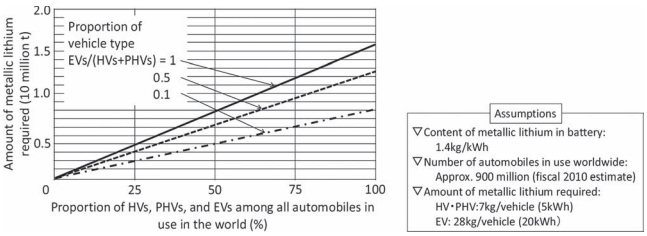

Figure 1. Predicted demand for metallic Li according to the portion of EV, HV, and PHV in the world market. Reproduced with permission.[9] Copyright 2011, National Institute of Science and Technology Policy.

electrochemical properties of the electrode materials. Therefore, the major challenge in advancing NIB technology lies in finding good electrode materials. An obvious place to look for good Na electrode materials is by starting at structures and chemistries that function well for Li intercalation. This is because the open crystal structure that allows Li intercalation is often suitable for Na intercalation. Furthermore, recently various Na compounds have been mimicked to investigate LIB electrode materials (i.e., Na_2FePO_4F).[16] This indicates that one can discover new electrode materials for NIB learning from LIB or vice versa. However, it is also clear that this strategy will not be sufficient as clear differences in behavior have been observed for the Na and Li equivalent of a compound. Specifically, layered $NaMO_2$ (M = V, Cr, Mn, Fe) showed more than half of the theoretical capacity reversibly, while their Li equivalents, $LiMO_2$, showed nearly no discharge capacity after first charge.[15,17–22] In this article, we briefly review some of the electrode materials that have been tested for NIB, especially focusing on recent developments. For the anode materials we distinguish carbonaceous and non-carbonaceous materials. For the cathode side we discuss separately oxide compounds, polyanion compounds, and other positive electrode compounds. The practical specific capacity and operation voltage of these materials are summarized in **Figure 2**.

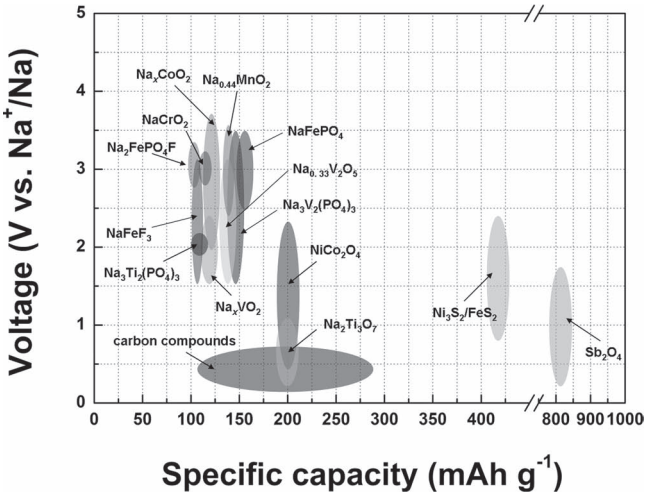

Figure 2. Electrode materials and corresponding electrochemical performances in current NIB technologies. Reproduced with permission.[46] Copyright 2011, American Chemical Society.

Kisuk Kang is Professor of Materials Science and Engineering at Seoul National University where he received his BS. His PhD at MIT was on the design of electrode materials for lithium batteries. Before he joined SNU, he was a professor at KAIST, Korea. His research lab at SNU focuses on developing new materials for LIB or post-Li battery chemistries—such as Na, Mg batteries and metal-air batteries—using combined experiments and ab-initio calculations.

Gerbrand Ceder is Professor of Materials Science and Engineering at MIT. His research interests lie in the design of novel materials for energy generation and storage. He has worked for over 16 years in the Li-battery field, optimizing several new electrode materials, and has published over 285 scientific papers. Dr. Ceder founded the Materials Genome Project, Computational Modeling Consultants, and Pellion Technologies, and his most recent scientific achievement is the development of materials for ultra-fast battery charging.

2. Negative Electrode Materials

2.1. Carbon Compounds

Graphite is the most common negative electrode material used in current LIB technologies.[3] Li readily forms intercalated compounds with graphite in which Li is located at the graphene inter-layer until the C:Li ratio reaches 6:1 (LiC_6).[23,24] The intercalation kinetics of Li ion in LIB is reasonably fast, hence the practical capacity (>360 mAh g^{-1}) of the graphite electrode almost approaches the theoretical capacity (372 mAh g^{-1}).[25] However, only a limited amount of Na can be stored in graphite.[26,27] Early first principles calculations indicated that it is hard for Na to form the intercalated graphite compounds compared to other alkali metals.[24]

In late 1970s and early 1980s, electrochemical alkali metal intercalation into graphite was studied with organic electrolytes. However, solvent cointercalation was problematic.[27,28] Hence, research on electrochemical Na insertion into carbon compounds was done by using solid electrolytes.[29] In 1993, Doeff *et al.* surveyed Na insertion properties of various carbon compounds (graphite, petroleum coke, and Shawinigan black) in

Na-cells with the solid electrolyte.[29] Only a small amount of Na ions could be inserted into a graphite electrode (~NaC_{70}), but much more Na could be inserted into petroleum coke (NaC_{30}) and Shawinigan black (NaC_{15}). The inserted Na ions were also reversibly extracted from the carbon electrode. In addition, a NIB full-cell was demonstrated using petroleum coke as a negative electrode and $Na_{0.6}CoO_2$ as a positive electrode. Although only half the capability of the positive electrode was achieved in that study, it is noteworthy that it demonstrated the feasibility of NIB system.

Thomas et al. investigated the electrochemical properties of graphite and carbon fibers in a carbonate-based liquid electrolyte ($NaClO_4$ in ethylene carbonate), with which the solvent cointercalation did not occur.[30] This study demonstrated that electrochemical insertion of Na into carbonaceous materials can reversibly take place in liquid electrolytes. All of the electrode materials showed large irreversible capacities at the first discharge. Significant portions of the irreversible capacities were associated with formation of passivation layers on the carbon surface. Elastic energy loss spectroscopy study identified that the layers were composed of Na_2CO_3 (formed near 0.8–1 V) and Na alkylcarbonates, $ROCO_2Na$ (formed below 0.8 V). The irreversible capacity of graphite was larger than that of the carbon fibers due to the higher specific area. Reversible capacities of carbon fibers and graphite were low (55 and 14 mAh g^{-1}, respectively). After grinding the carbon fibers, the reversible capacity was increased to 83 mAh g^{-1} (NaC_{26}).

Na showed better reactivity with other types of carbon compounds such as cokes and carbon blacks. As a result, a variety of non-graphitic carbon compounds were investigated as negative electrode materials.[23,29,31–38] The Na reaction voltage with non-graphitic carbon compounds typically shows two distinct voltage regions as shown in **Figure 3**. Initial reaction with Na gives a sloping voltage profile (region I) which is followed by a low voltage plateau region (II) near 0 V.[23,38,39] Steven et al. investigated the Na storage mechanism of carbon compounds

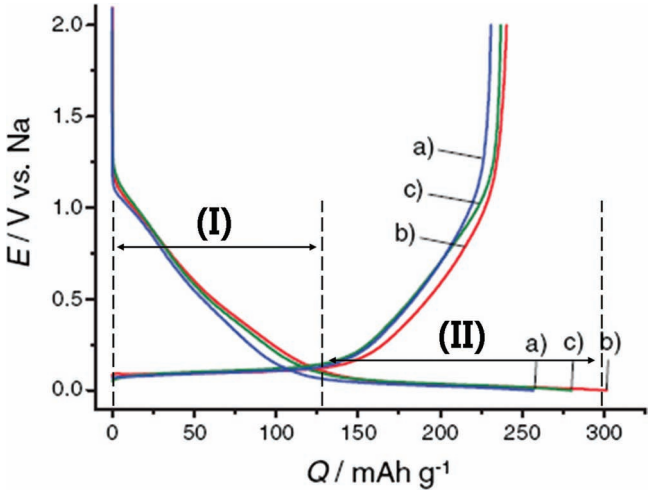

Figure 3. Typical charge-discharge profiles of carbon electrodes in organic electrolytes: hard carbon electrodes cycle in (a) ethylene carbonate electrolyte, (b) propylene carbonate electrolyte, and (c) butyl carbonate electrolyte. Reproduced with permission.[38]

with in-situ scattering study.[23,39] They revealed that the plateau region (II) corresponded to the filling of pores in the carbons. The Na chemical potential in the pore filling is close to that of the elemental Na metal, resulting in a voltage near 0 V. On the other hand, the sloping voltage in (I) originates from Na intercalation into graphene inter-layers. In the carbon compounds, disordered graphene layers are randomly distributed, thus, Na chemical potentials intercalating into graphene inter-layers vary continuously resulting in sloping voltage region. Na intercalation was identified by detecting the inter-layer distance of the graphene stacking. The inter-layer distance increased when discharged and decreased when charged, indicating that Na reversibly intercalated and deintercalated during the reaction. A nuclear magnetron resonance (NMR) study has also revealed the reversible insertion of Na in the carbon compounds.[34]

Since 2000, many researchers have continuously proposed high-capacity carbon compounds for NIB.[23,31–35,38,40,41] For examples, pyrolized glucose and carbon microspheres showed high reversible capacities of 300 and 285 mAh g^{-1} in a Na-cell, respectively.[34,36] Carbon black delivered 200 mAh g^{-1} in a full cell with $Na_{0.7}CoO_2$ counterpart.[37] However, these studies were performed with relatively low current rates and, sometimes, at elevated temperatures. Recently, high rate-capable carbon electrode was reported using a templated carbon.[41] The templated carbon was prepared *via* infiltrating mesophase-pitch into a porous silica template. The templated carbon has a hierarchical micro-structure with interconnected pores as shown in **Figure 4**a. The templated carbon showed a high specific capacity (130 mAh g^{-1}, NaC_{17}) at relatively high current rate of 74.4 mA g^{-1} as shown in Figure 4b. At even higher current rates (744 and 1860 mA g^{-1}), more than 100 mAh g^{-1} capacity could still be obtained. The authors stated that the kinetics of Na insertion into carbon electrodes was improved due to the structure of the templated carbon, where the interconnected pore structure minimized the diffusion lengths and the carbon microstructure enhanced electronic conductivity. However, a clear understanding of the relationship between the reversible capacity and carbon microstructure (including porosity) is not yet established. Nevertheless, it is worth noting that control of the carbon microstructure is a viable strategy to improve the performance of carbon negative electrodes. More recently, Komaba et al. reported high rate performance of hard carbon in a full-cell with $NaNi_{0.5}Mn_{0.5}O_2$ positive electrode.[38] The specific capacity at the first cycle was about 250 mAh g^{-1} at a high current rate of 300 mA g^{-1} (based on weight of hard carbon). After 50 cycles, the specific capacity was still above 150 mAh g^{-1}.

Given that battery safety is in part determined by the electrode materials, Xia et al. compared the thermal stabilities of sodiated hard carbon and lithiated mesocarbon microbeads (MCMB) in various organic solvents with and without $NaPF_6$ (or $LiPF_6$) salt.[35] The onset temperatures of self-heating of the lithiated MCMB and the sodiated hard carbon were comparable in the salt-free ethylene carbonate:diethyl carbonate (EC:DEC) solvent. However, dissolving $NaPF_6$ salt increased the reactivity of the sodiated hard carbon, resulting in a decrease in the onset temperature and increase in the heating rate. Dissolving $LiPF_6$ salt into EC:DEC significantly reduced the reactivity of the lithiated MCMB due to the formation of stable LiF phases in the passivation layers at

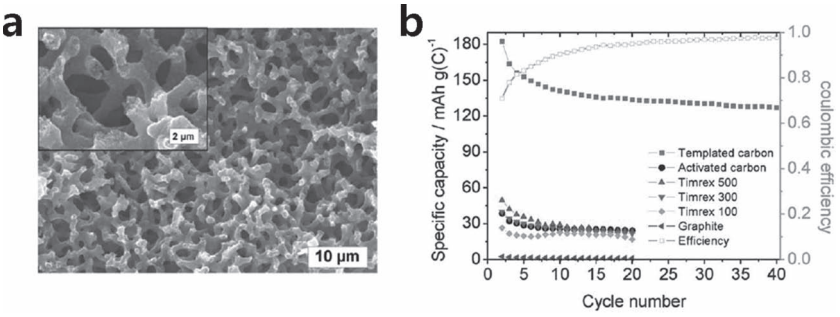

Figure 4. (a) Microstructure of templated carbon and (b) capacity retention of various carbon compounds at 74.4 mA g^{-1} in Na-cell. Reproduced with permission.[41] Copyright 2011, Royal Society of Chemistry.

elevated temperature. After the thermal test of the sodiated hard carbon, Na methyl carbonate with minor NaF phase was detected at the surface. Since $NaPF_6$ has higher thermal stability than $LiPF_6$, only a small amount of $NaPF_6$ was decomposed to NaF. Thermal stability of the sodiated hard carbon was also affected by types of organic solvents, implying that finding an adequate Na salt and suitable solvent composition is important for the stability of NIB.

2.2. Non-Carbon Compounds

Non-carbonaceous negative electrode materials have also been pursued as possible negative electrode materials. Various intercalation compounds, conversion compounds, and alloying compounds have been suggested as anode materials for NIB.[19,42–48] The reaction mechanism of these compounds are similar to those of LIB negative electrode materials and are briefly illustrated in **Figure 5**.[7]

Recently, Ti-based intercalation compounds were investigated due to the relatively low redox potentials of $Ti^{3+/4+}$. Several Ti-based Na compounds have been shown to reversibly intercalate Na.[46,49,50] Layered $NaTiO_2$ electrode is electrochemically active with 0.3–0.5 Na transfer (depending on cut-off voltage) around 1 V.[49] Recently, reversible reaction in $Na_2Ti_3O_7$ has been reported at significantly lower voltage.[46] Two Na ions could be inserted into $Na_2Ti_3O_7$ (0.67 Na per Ti, 200 mAh g^{-1}). A reversible phase transition is found to occur between $Na_2Ti_3O_7$ and a $Na_{12}Ti_{10}O_{28}$-like $Na_4Ti_3O_7$ phase during the electrochemical reaction with a voltage of approximately 0.3 V, which is the lowest voltage ever reported for an oxide electrode in NIB. $NaTi_2(PO_4)_3$ was investigated as the negative electrode in aqueous NIB.[50] It showed a specific capacity of 130 mAh g^{-1} with a 2.1 V plateau in a Na-cell with an organic electrolyte.

Conversion compounds such as CoO, Co_3O_4, CuO, and Cr_2O_3 have been extensively studied in LIB due to their high specific capacities.[5,7,51,52] The conversion reaction in LIB is expressed by the following equation:

$$nLi^+ + ne^- + M^{n+}X = Li_nX + M^0 \quad (1)$$

where M is a transition metal, X is an anion, and n is the oxidation number of the transition metal ion in MX. A multiple electron reaction is possible per transition metal, leading to high theoretical specific capacity. In 2002, Alcátara et al. indicated that Na can also induce conversion reactions of a transition metal oxide.[42] The electrochemical properties of spinel $NiCo_2O_4$ electrodes were examined in Na-cell and Li-cells.[42,53] The theoretical capacity of $NiCo_2O_4$ is approximately 890 mAh g^{-1} based on the assumption that 8 Na react with $NiCo_2O_4$ to form Ni, 2

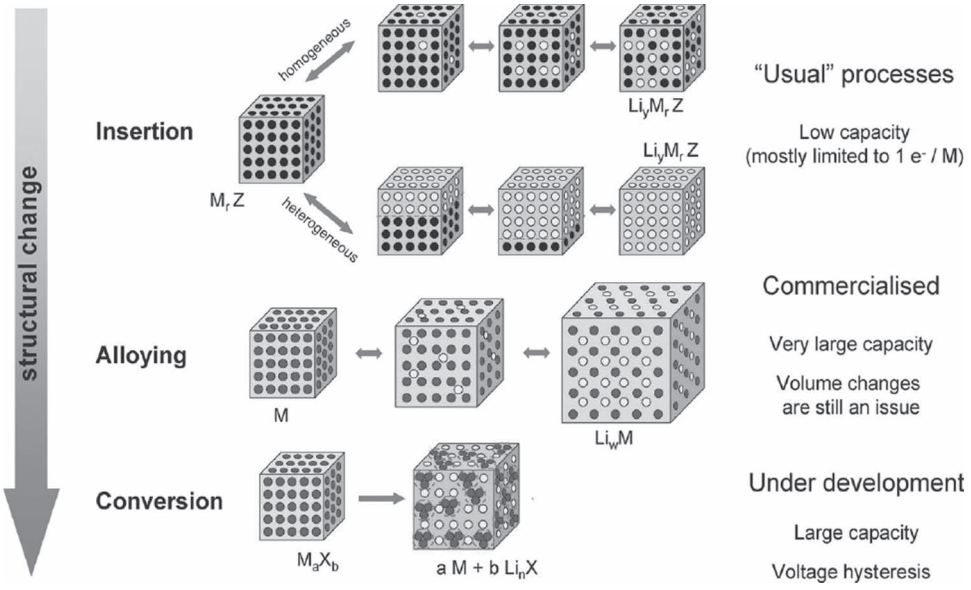

Figure 5. Schematic illustration of the reaction mechanisms of electrode materials with Li ions in LIB. Reproduced with permission.[7] Copyright 2009, Royal Society of Chemistry.

Co, and 4 Na_2O via the conversion reaction. However, $NiCo_2O_4$ in a Na-cell delivered lower reversible capacity of ~200 mAh g^{-1} and showed abnormally large capacity at the first discharge due to the electrolyte degradation at low voltage. Nevertheless, the electrochemical property obtained from a full-cell ($NiCo_2O_4$// $Na_{0.7}CoO_2$) seemed more promising (~250 mAh g^{-1} based on the weight of $NiCo_2O_4$ electrode, higher than the carbon negative electrode). Sulfide compounds, such as FeS_2 and Ni_3S_2, have also been investigated as negative electrodes for NIB[54–57] and form Na_2S and nanosized metal particles as a result of the conversion reaction. On the contrary, FeO, CoO, and NiO showed almost no electrochemical activity with Na, while they exhibited excellent performances via the conversion reaction in Li-cells.[47,58] The reason why the same material shows different electrochemical activity with Li and Na is not clearly understood yet.

Metals, which form alloys with Na, can electrochemically store Na ions by alloying ($M + nNa^+ + ne^- = Na_nM$) in NIB.[43] The alloying reaction of Pb to form $Na_{3.75}Pb$ in a Na-cell was reported in reference [59] Electrochemical alloying of Sn-Na was also reported in a study on Sb_2O_4 thin film.[47] Sodiation of Sb_2O_4 leads to conversion followed by alloying. Sb_2O_4 has a high specific capacity (theoretical capacity = 1227 mAh g^{-1}) as a total of 14 Na ions can be stored per formula unit of Sb_2O_4 by the following reactions:

$$Sb_2O_4 + 8Na^+ + 8e^- = 2Sb + 4Na_2O \quad (2)$$

$$2Sb + 6Na^+ + 6e^- = 2Na_3Sb \quad (3)$$

The reversible capacity of the Sb_2O_4 thin film electrode was approximately 896 mAh g^{-1}, which is the highest capacity among various negative electrode candidates achieved so far.

In spite of high specific capacity of the conversion compounds and alloying compounds, their utilizations are still challenging due to their significant volume change upon charge and discharge. Chevrier et al. evaluated a relationship between volumetric energy density and volume expansion in the alloying compounds using first principles calculations as shown in **Figure 6**.[43] The Na alloying compounds possess about two-fold lower capacity density compared to Li alloying compounds at the same volume expansion rate. This is because the ionic radius of Na is considerably larger than that of Li. Note that in order to reach the capacity of conventional graphite in LIB, the Na alloying compounds should experience about 150% of volume expansion. This indicates the challenges in utilizing conversion or alloying compounds as the negative electrode.

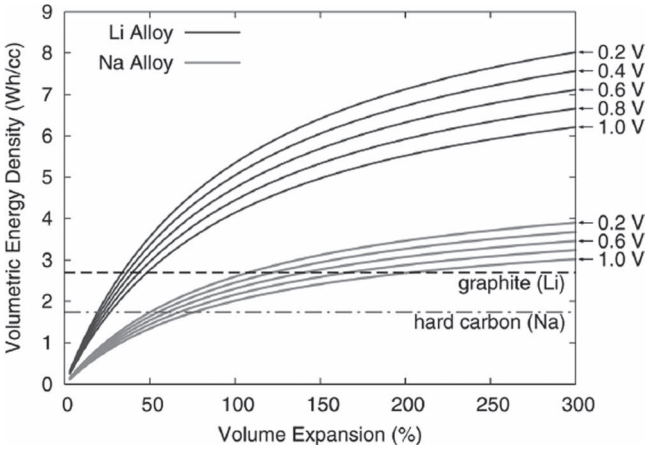

Figure 6. Universal expansion curves for Li and Na alloys. Voltage of positive electrode was assumed to be 3.75 V to calculate the energy density. Reproduced with permission.[43] Copyright 2011, The Electrochemical Society.

3. Positive Electrode Materials

3.1. Oxide Compounds

Layered $LiMO_2$ compounds have been extensively investigated as Li-intercalation materials. Hence, it is no surprise that similar $NaMO_2$ compounds have been targeted as Na-intercalation electrodes.[19,60–63] Layered Na_xMO_2 possesses various crystal structures. In the notation of Delmas et al.,[64] O*n* (*n* = 1, 2, 3, etc.) refers to structures in which Na is octahedrally coordinated by oxygen, and *n* refers to the repeat period of the transition metal stacking. Na atoms can also occupy trigonal prismatic sites and these structures are noted as P*n*.[65] Phase transitions between P*n* and O*n* occur via the gliding of MO_2 sheets. Such gliding of oxygen layers with respect to each other has been observed at room temperature. For example, O3-$NaCoO_2$ can transform into a P'3 structure during electrochemical desodiation.[60] However, phase transitions between P*n* and O*m* ($m \neq n$) need to break M-O bonds, and are only possible at high temperatures.[66] Due to this competition between P and O type arrangements the desodiation behavior of layered Na-compounds is in many cases not fully topotactic. Very little is understood how these gliding transitions occur and what their effect on the kinetics of sodiation/desodiation is. As Li atoms usually do not occupy trigonal prismatic sites, these gliding transitions are not an issue in layered Li-intercalation compounds. But Na-compounds may also have advantages. In layered Li_xMO_2 compounds the competition usually exists with structures in which the Li ion is tetrahedrally coordinated leading to the formation of spinel-like structures with accompanying loss in capacity.[18,67–69] Such a driving force towards spinel formation will less likely be present for Na-intercalation compounds, making it possible that they are stable over a larger concentration range of alkali.

In 1981 Delmas et al. showed that the phase transition of various Na_xCoO_2 structures occurred reversibly in electrochemical Na-cells, demonstrating the feasibility of Na_xCoO_2 as a positive electrode material.[60] Various crystal structures of Na_xCoO_2 compounds are illustrated in **Figure 7**a–c. Among those, P2-$Na_{0.70}CoO_2$ showed the largest energy density (~260 Wh kg^{-1}) in NIB. Recently, P2-Na_xCoO_2 has been reinvestigated,[70,71] and found to reversibly operate between $0.45 \leq x \leq 0.90$, when $Na_{0.74}CoO_2$ was used as the starting material. The existence of several well defined steps in the voltage profile indicated that various structures were formed during the cycling (**Figure 8**a). The formation of Na-vacancy ordered layer-structures was confirmed via in-situ X-ray diffraction study.[70,72] The feasibility of using P2-Na_xCoO_2 as the positive electrode in an all solid-state NIB was also recently demonstrated.[71]

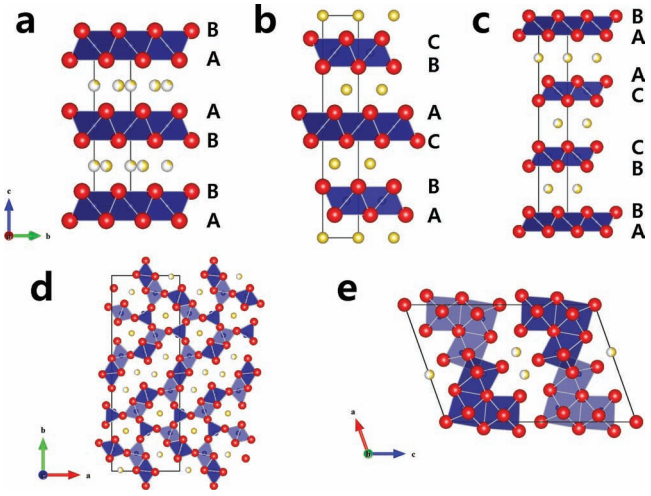

Figure 7. Crystal structures of various Na_xMO_y: (a) P2-Na_xCoO_2, (b) O3-Na_xCoO_2, (c) P3-Na_xCoO_2, (d) $Na_{0.44}MnO_2$, and (e) $Na_{0.33}V_2O_5$ (Na: yellow, Co/Mn/V: blue, O: red).

Analogues of P2-Na_xCoO_2 were suggested including Mn-substituted P2-$Na_{2/3}Co_{2/3}Mn_{1/3}O_2$, in which Co^{3+} and Mn^{4+} coexist.[73] While P2-$Na_{2/3}CoO_2$ showed several voltage steps in discharge, the Mn-substituted P2-$Na_{2/3}Co_{2/3}Mn_{1/3}O_2$ electrode showed only one step at $Na_{1/2}Co_{2/3}Mn_{1/3}O_2$ composition (Figure 8a). Similar to P2-$Na_{2/3}CoO_2$, P2-$Na_{0.6}MnO_2$, exhibited several voltage steps upon cycling.[74] These P2-$Na_{2/3}Co_{1-x}Mn_xO_2$ compounds all retained the P2 framework upon the cycling. On the other hand, P2-$Na_{2/3}Ni_{1/3}Mn_{2/3}O_2$ undergoes different phase transition.[75] During Na extraction, O2-type stackings form in the P2-$Na_xNi_{1/3}Mn_{2/3}O_2$ when x reaches ~1/3. P2-$Na_{1/3}Ni_{1/3}Mn_{2/3}O_2$ (with some O2-type stackings) and O2-$Ni_{1/3}Mn_{2/3}O_2$ phases coexist when x is lower than 1/3. The original P2 phase was reversibly recovered after the discharge. All of these P2 compounds could deliver about 0.5 Na ions, resulting in a specific capacity of 120–150 mAh g^{-1}.

Layered materials with composition $NaMO_2$ seem to be more promising. $NaMO_2$ compounds generally form an O3 structure as illustrated in Figure 7b.[21,61,76] Early work on $NaMO_2$ reported that only a small amount of Na ions (~0.2) participated in the

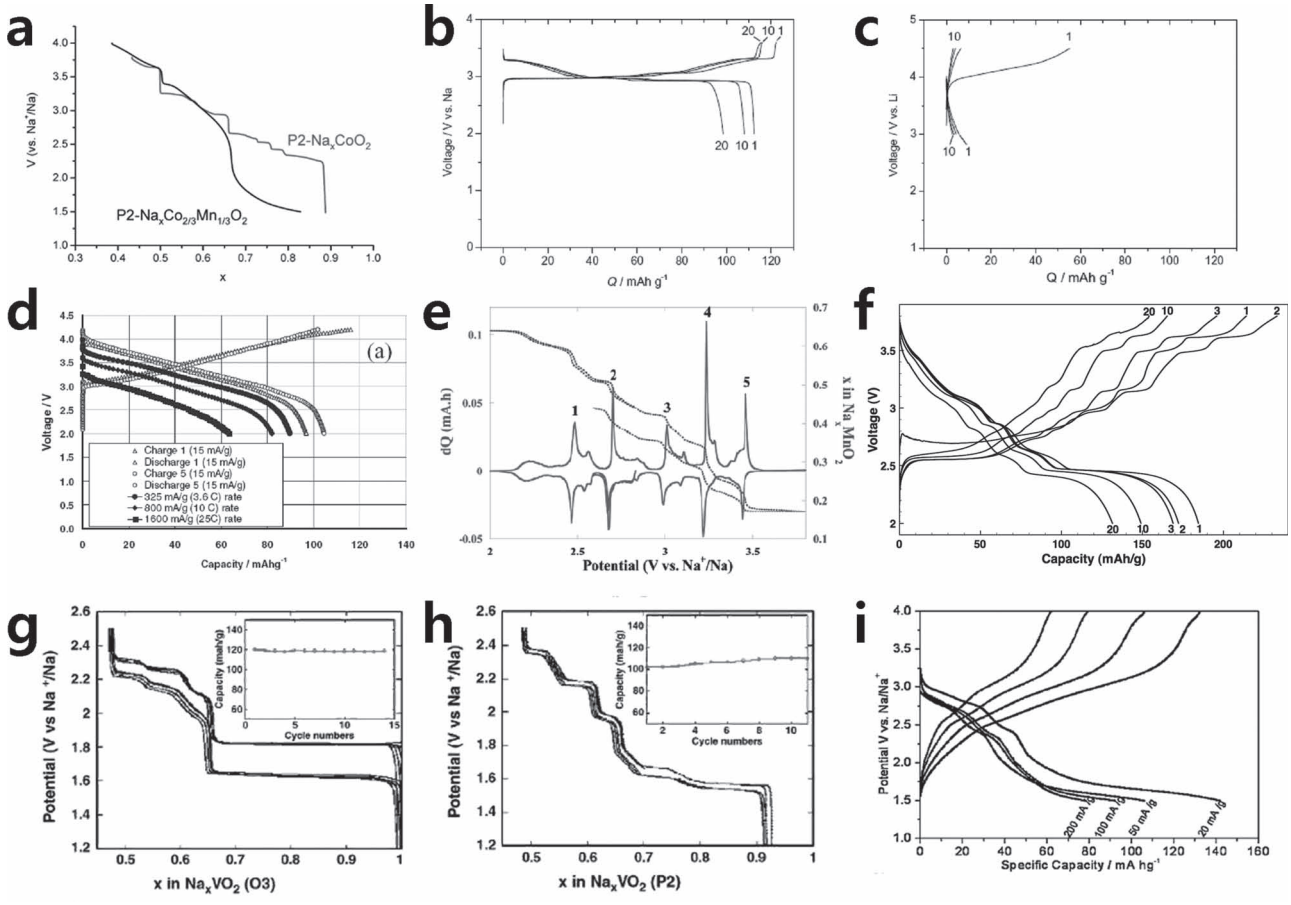

Figure 8. Charge-discharge profiles of various oxide compounds: (a) (black) P2-Na_xCoO_2 and (blue) P2-$Na_xCo_{2/3}Mn_{1/3}O_2$, (Reproduced with permission.[73] Copyright 2011, Royal Society of Chemistry.), (b) $NaCrO_2$, (c) $LiCrO_2$ (Reproduced with permission.[18] Copyright 2010, Elsevier.) (d) $Na_{1.0}Li_{0.2}Ni_{0.25}Mn_{0.75}O_{2.35}$ (Reproduced with permission.[80]), (e) $Na_{0.44}MnO_2$ (Reproduced with permission.[62] Copyright 2007, American Chemical Society.), (f) $NaMnO_2$, (Reproduced with permission.[15] Copyright 2011, The Electrochemical Society.) (g) $NaVO_2$, (h) $Na_{0.7}VO_2$ (Reproduced with permission.[44] Copyright 2011, Elsevier.) and (i) $Na_{0.33}V_2O_5$ (Reproduced with permission.[96] Copyright 2010, Elsevier).

electrochemical reaction for $NaCrO_2$ and $NaNiO_2$ electrodes resulting in low specific capacities.[61] However, when $NaCrO_2$ was recently revisited, ~120 mAh g^{-1} (~0.5 Na) of capacity near 3 V was obtained (Figure 8b).[18,63] It is interesting that $NaCrO_2$ shows much better performance than $LiCrO_2$ in (<10 mAh g^{-1}) as shown in Figure 8b-c. The authors of Ref [18] speculate that bonding distances strongly affect the reactivity of the two compounds. The size of the inter-slab interstitial tetrahedral sites in $LiCrO_2$ lattice is well matched to the stable configuration of $Cr^{4+}O_4^{2-}$ tetrahedral, hence Cr^{4+}, formed during charge, easily migrates and gets trapped in the tetrahedral sites. However, the interstitial sites in $NaCrO_2$ lattice cannot stabilize the Cr^{4+} due to large inter-slab distance and oxygen-oxygen bonding length preventing the migration of Cr^{4+}.

In Li-cells, $LiNi_{0.5}Mn_{0.5}O_2$ can deliver over 200 mAh g^{-1} at low rate,[77,78] and high rate $LiNi_{0.5}Mn_{0.5}O_2$ can be made by ion-exchange from $NaNi_{0.5}Mn_{0.5}O_2$.[79] When directly testing in Na cells, the layered $NaNi_{0.5}Mn_{0.5}O_2$ delivered 130 mAh g^{-1}.[38,63] Almost no alkali-Ni disordering occurs in the Na version of the compound, in contrast to Ni-containing layered Li compounds which have considerable disorder. The better ordering of the Na compound is due to its larger ionic size.[79] Electrochemical desodiation and subsequent lithiation of $NaFeO_2$ was observed in a hybrid Li-cell.[21] The reaction was reversible until charged to $Na_{0.5}FeO_2$, but irreversible reaction occurred with further electrochemical oxidation.

Recently, Kim et al. suggested Li-substituted $Na_{1.0}Li_{0.2}Ni_{0.25}Mn_{0.75}O_{2.35}$ (or $Na_{0.85}Li_{0.17}Ni_{0.21}Mn_{0.64}O_2$) as the positive electrode material.[80] In this composition, the (Ni+Mn)/(Na+Li) ratio was 1/1.2, and thus, this compound can be regarded in the family of alkali-excess materials like $Li_{1.2}Ni_{0.2}Mn_{0.6}O_2$.[67,81,82] Due to the difference in ionic radius of Na and Li, Na ions are located in the inter-slab spaces, while the excess-Li ions are located in the transition metal layers. The electrochemical reaction in these materials is fully supported by the two-electron reaction of the $Ni^{2+/4+}$ redox couple with the oxidation state of Mn ions (+4) remaining unchanged which imparts stability to these materials. This behavior is frequently observed in Ni^{2+}-Mn^{4+} containing compounds such as $LiNi_{0.5}Mn_{0.5}O_2$ and $Li_{1.2}Ni_{0.2}Mn_{0.6}O_2$ electrodes in LIB.[79,83,84] The specific capacity and average voltage was approximately 100 mAh g^{-1} and 3.4 V, respectively (Figure 8d). It was claimed that the excess Li ions stabilize the crystal structure upon cycling.

There exists a variety of stable manganese-based oxides, which are composed of one-, two-, or three-dimensionally connected sites for alkali metal intercalations.[85] Tarascon et al. reported electrochemical Na intercalation into spinel λ-MnO_2.[86] When Na ions were inserted into λ-MnO_2 at the first discharge, the spinel phase transformed to a new layered structure. After this irreversible phase transition, almost 0.6 Na ions could reversibly cycle. Co-substituted $Mn_{2.2}Co_{0.27}O_4$ also showed electrochemical activity with up to one Na ion transfer.[87] Orthorhombic $Na_{0.44}MnO_2$ (or $Na_4Mn_9O_{18}$) possesses a 3D tunnel structure as illustrated in Figure 7d.[62,88–90] Figure 8e shows that reversible Na storage reaction takes place for $0.18 \le x \le 0.64$ (~140 mAh g^{-1}) in Na_xMnO_2.[62] By nanosizing $Na_{0.44}MnO_2$, promising electrochemical properties were obtained in both a Na-cell and full-cell with pyrolyzed carbon as a negative electrode.[80] Stable electrochemical reaction in an aqueous electrolyte has also been demonstrated for this material.[91] Recent results showed that O3-$NaMnO_2$ exhibits 185 mAh g^{-1} discharge capacity for the first cycle at C/10 rate with 132 mAh g^{-1} remaining after 20 cycles (Figure 8f).[15] O3-$NaMnO_2$ shows remarkably different electrochemical properties from O3-$LiMnO_2$, which transforms into a spinel-like structure with a rapid capacity decay during cycling.[17,92]

O3-$NaVO_2$ electrodes could deliver a specific capacity of ca. 120 mAh g^{-1} (~0.5 Na) reversibly at 1.4–2.5 V.[19] When approximately 0.9 Na was extracted with higher voltage (~3 V), irreversible phase transition occurred and only a small amount of Na (~0.4 Na) was re-inserted at subsequent discharge. Hamani et al. reported that $Na_{0.7}VO_2$ showed much less polarization than $NaVO_2$ as shown in Figure 8g and h.[44] The original structure of P2-$Na_{0.7}VO_2$ electrode was well retained during cycling without drastic structural change. High electronic conductivity of P2-$Na_{0.7}VO_2$ is believed as the origin of the reduced polarization while O3-$NaVO_2$ is electronically insulating. Na_xVO_2 with low redox potential (<2.5 V) is sensitive to air exposure. $NaVO_2$ readily decomposes to Na_xVO_2 and Na_2O when exposed to air. However, V compounds with higher oxidation state ($V^{4+/5+}$) such as V_2O_5, $Na_xV_2O_5$, and $Na_{1+x}V_3O_8$ are stable in air and can be operated above 3 V.[93–96] Among those, $Na_{0.33}V_2O_5$ (in Figure 7e) nanorods showed good electrochemical behavior with 142 mAh g^{-1} discharge capacity at 1.5–4.0 V range (Figure 8i).[96]

3.2. Polyanion Compounds

In the past decade, extensive research efforts have been focused on polyanion compounds for positive electrode materials in LIB.[4,97] Polyanion compounds provide some advantages.[97] Various crystal structures with open channels for Na and Li ions are available.[97] Since the operation voltage is influenced by local environments of polyanions, the operation voltage of a specific redox couple can be tailored.[98] In addition, the polyanion compounds are believed to have high thermal stabilities due to strong covalent bonding of oxygen atom in the polyanion polyhedra, though this may not be universally true.[99,100] A recent high-throughput computational study evaluated on a large scale the properties of phosphate compounds for LIB.[101] Some Na compounds with the polyanion frameworks have been studied to be used as structural motifs and starting materials for hybrid Li-cells, or to compare the electrochemical properties with isostructural Li compounds. Crystal structures of various polyanion compounds are described in **Figure 9**.

NASICON, Na super-ionic conductor, whose general formula is $A_xMM'(XO_4)_3$, was originally studied as a solid electrolytes that allows fast Na ion conduction through the empty space in its crystal structure.[102–104] Corner-shared MO_6 (or $M'O_6$) and XO_4 polyhedra form a framework with large Na diffusion channels. NASICON compounds were studied as solid electrolytes in Na-S batteries for a long time. In 1987 and 1988, Delmas et al. demonstrated that NASICON-type compounds, $NaTi_2(PO_4)_3$, can be electrochemically active with Na in a reversible manner.[102,104] Since then, NASICON-type compounds (transition metal = V, Fe, Ti, and etc) were investigated for both LIB and NIB, however, most work was focused on LIB due to poor cell performance in NIB.[105–107] Recently, carbon-coated $Na_3V_2(PO_4)_3$

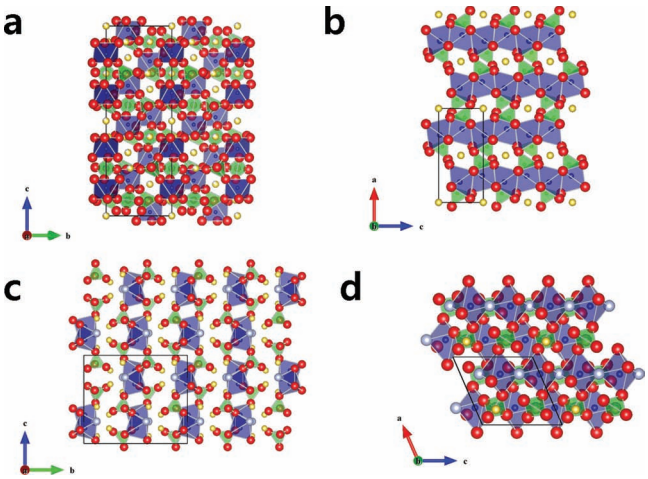

Figure 9. Crystal structures of various polyanion compounds: (a) $Na_3V_2(PO_4)_3$, (b) $NaFePO_4$, (c) Na_2FePO_4F, and (d) $NaFeSO_4F$ (Na: yellow, V/Fe: blue, O: red, F: gray).

(structure illustrated in Figure 9a) was investigated and showed promising performance as a NIB electrode material. In the electrochemical profiles of $Na_3V_2(PO_4)_3$ shown in **Figure 10**a-b, two distinct plateaus near 1.63 and 3.40 V were identified, which are related to the $V^{2+/3+}$ and $V^{3+/4+}$ redox couple, respectively. Using a voltage range of 2.7–3.8 V, a reversible capacity of 93 mAh g^{-1} was obtained with excellent cyclability. The lower voltage region (1.0–3.0 V) delivered about 59 mAh g^{-1} capacity with good cycle performance. Taking advantage of the big voltage difference between the plateaus, a symmetric cell using $Na_3V_2(PO_4)_3$ as both negative and positive electrodes was designed with an ionic liquid electrolyte.[108] The symmetric cell reversibly delivered 64 mAh g^{-1}. F-containing V-based polyanion compounds such as $NaVPO_4F$, $Na_3V_2(PO_4)_2F_3$, and $Na_{1.5}VOPO_4F_{0.5}$ have also been investigated in NIB. The crystal structures of F-containing compounds are comparable to those of the NASICON structure.[109–111] $Na_{1.5}VOPO_4F_{0.5}$ delivered about 0.56 Na in Na-cells with two voltage plateaus near 3.6 and 4.0 V.[111] A full-cell composed of hard carbon and $NaVPO_4F$ exhibited reversible capacity about 80 mAh g^{-1} with 3.7 V average voltage.[109]

$LiMPO_4$ (M = Fe, Mn, Co, Ni) is the most common polyanion electrode in LIB.[112–114] Conversely, only a few reports were published for electrochemical characterization of $NaMPO_4$ for NIB because maricite $NaMPO_4$, which is thermodynamically more stable than olivine $NaMPO_4$, is almost inactive with Na deintercalation due to the absence of adequate Na diffusion channel.[115–117] Meta-stable olivine $NaFePO_4$ phase (Figure 9b) could be obtained by delithiation and subsequent sodiation of the olivine $LiFePO_4$.[116,118] $NaMn_{1-x}M_xPO_4$ (M = Fe, Ca, Mg) can be synthesized via topochemical synthesis starting from $NH_4Mn_{1-x}M_xPO_4 \cdot H_2O$.[118] It is well-known that de/intercalation of Li in olivine compounds occurs via two-phase reaction between Li-deficient Li_xMPO_4 and Li-rich $Li_{1-x}MPO_4$ (x~0),

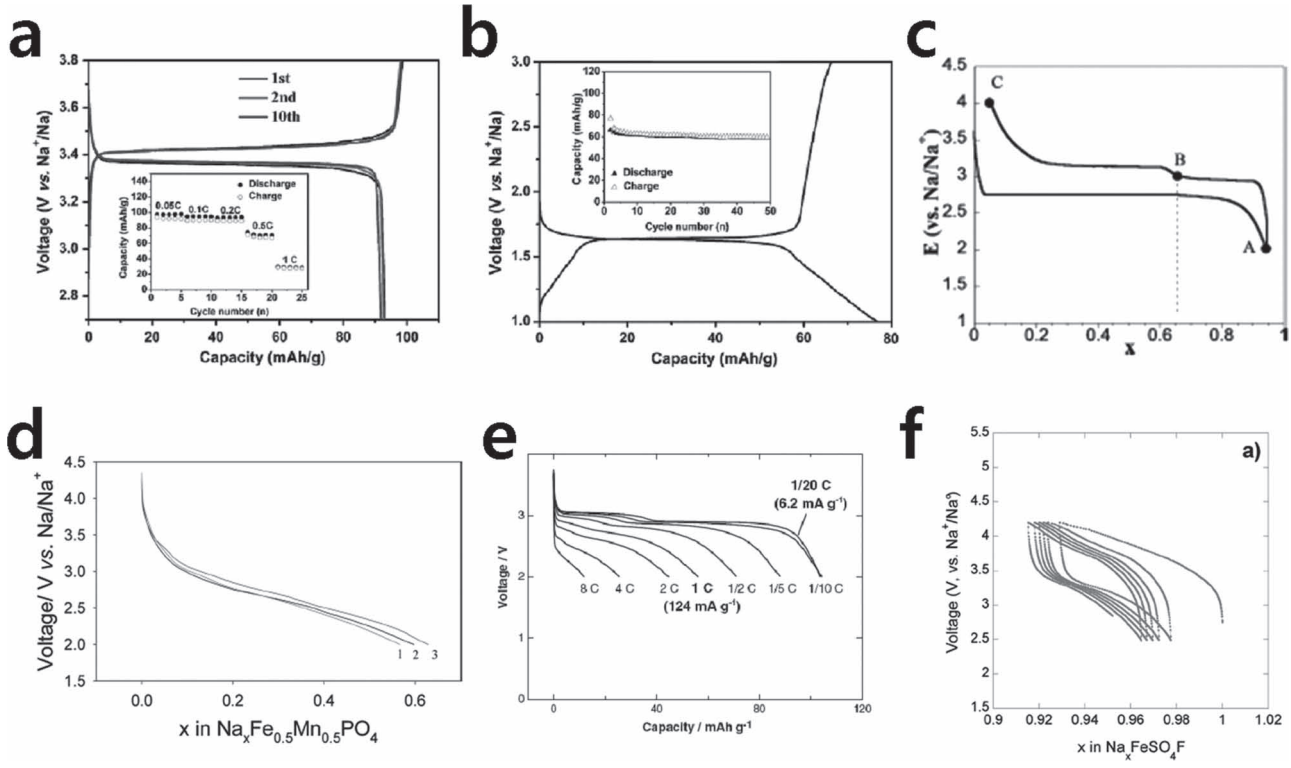

Figure 10. Electrochemical profiles of various polyanion compounds in Na-cells: (a) $Na_3V_2(PO_4)_3$ at high voltage region, (b) $Na_3V_2(PO_4)_3$ at low voltage region (Reproduced with permission.[141] Copyright 2011, Elsevier.), (c) $NaFePO_4$ (Reproduced with permission.[116] Copyright 2010, American Chemical Society.), (d) $NaMn_{0.5}Fe_{0.5}PO_4$ (Reproduced with permission.[118] Copyright 2011, American Chemical Society.), (e) Na_2FePO_4F, (Reproduced with permission.[126] Copyright 2011, Elsevier.), and (f) $NaFeSO_4F$. (Reproduced with permission.[123] Copyright 2010, American Chemical Society.)

except for some special cases.[98,119–121] Interestingly, de/intercalation of Na in olivine $NaFePO_4$ and $NaMn_{0.5}Fe_{0.5}PO_4$ did not follow the conventional behavior (Figure 10c-d).[116,118] When discharging olivine $FePO_4$, a distinct step in the discharge profile was observed near 2.95 V, which corresponds to the formation of a $Na_{0.7}FePO_4$ intermediate phase (Figure 10c).[116] The intermediate phase was also identified after chemical desodiation of $NaFePO_4$.[118] Approximately 0.9 Na ions were seen to reversibly react with an average voltage near 2.92 V in $NaFePO_4$. $NaMn_{0.5}Fe_{0.5}PO_4$, on the other hand, showed a single-phase reaction for all Na compositions[118] and displayed a sloping discharge profile without any voltage plateau (~0.6 Na ion reaction). Strain energy between the Na-rich and Na-deficient phases due to the large size of Na ion was speculated to be the origin of this behavior. Shiratsuchi et al. investigated electrochemical activity of $FePO_4$ electrodes with an amorphous or trigonal structure.[122] Amorphous $FePO_4$ electrodes (~120 mAh g^{-1}) showed better performance compared to the one with trigonal structure.

Recently, various $(PO_4F)^{4-}$ and $(SO_4F)^{3-}$ based Na compounds have been investigated in searching for new positive electrode materials in LIB.[123–130] While these Na compounds were mostly considered as structural motifs for Li compounds, some can be used as active electrodes for NIB. Na_2FePO_4F possesses a layered-like two-dimensional framework of $Fe_2O_7F_2$ bioctahedra connected by PO_4 tetrahedra with Na ions located in the inter-layer space as illustrated in Figure 9c. Ellis et al. confirmed that desodiation from Na_2FePO_4F to $NaFePO_4F$ did take place successfully *via* chemical oxidation, however, electrochemical properties in Na-cell were not shown in this study.[16] Recham et al. further investigated $Na_2Fe_{1-x}Mn_xPO_4F$ ($0 \le x \le 1$) in Na-cell.[131] While Na_2FePO_4F showed fair electrochemical activity to Na (~100 mAh g^{-1} with 3 V operation), Na_2MnPO_4F was almost inactive. Furthermore, the electrochemical activity of $Na_2Fe_{1-x}Mn_xPO_4F$ electrodes drastically decreased with increasing Mn content. This is coincident with a crystal structure change in $Na_2Fe_{1-x}Mn_xPO_4F$ depending on the Mn content. At~25% of Mn, the crystal structure of $Na_2Fe_{1-x}Mn_xPO_4F$ changes to a Na_2MnPO_4F-like structure, which is believed to be disadvantageous for Na ion conduction.[124,131] A Na_2FePO_4F electrode could deliver 110 mAh g^{-1} at 6.2 mA g^{-1}, but the capacity decayed drastically with an increase in the current density (60 mAh g^{-1} at 124 mA g^{-1}) as shown in Figure 10e. Recently, electrochemically active Na_2MnPO_4F was reported by size reduction and conductive carbon coating, however, this work was performed in a hybrid Li-cell.[132] Most work on Na_2MPO_4F has been done with hybrid Li-cells to show the possibilities of Li_2MPO_4F electrodes, hence, a clear understanding of the electrochemical activity of sodiation and desodiation in these materials is still missing.

Tavorite $LiFeSO_4F$ was reported to be a promising positive electrode material for LIB due to the multi-channel Li ion conduction.[125] $NaFeSO_4F$ is composed of almost same polyanion framework with $LiFeSO_4F$, but with slight difference in Li and Na positions.[123,129] While there are two distinguishable Li ion sites in $LiFeSO_4F$, only one Na ion site is available for $NaFeSO_4F$ (Figure 9d). Hence, $NaFeSO_4F$ ($P2_1/c$) has higher symmetry compared to $LiFeSO_4F$ (P-1). Barpanda et al. argued that $NaFeSO_4F$ (~7.14×10^{-7} S·m^2) had higher ionic mobility compared to $LiFeSO_4F$ (~7.0×10^{-11} S·m^2) through impedance spectroscopy on pellets.[123] A $NaFeSO_4F$ electrode was electrochemically active in a hybrid Li-cell, but showed little electrochemical activity (~0.08 Na ion transfer) in a Na-cell up to 4.2 V (Figure 10f).[123,125] Electrochemical Na intercalation into delithiated $FeSO_4F$ was not successful either. It was claimed that limited electronic conduction and large volume difference between $NaFeSO_4F$ and $FeSO_4F$ phases (~16%) might be the reason for poor electrochemical activity. A computational study on ionic diffusivity in both phases by Tripathi et al. suggested that $LiFeSO_4F$ has lower activation energy for the diffusion (~400 meV) in three-dimensional diffusion paths.[125] In contrast, only one-dimensional zigzag path for Na diffusion was possible for $NaFeSO_4F$ with relatively high activation energy of 600 meV. First principles calculations on $LiFeSO_4F$ indicate that the structure has a one-dimensional diffusion path for Li with very low activation barrier, but that diffusion in large particles may require access to a defect cross over mechanism between these one-dimensional paths, resulting in a higher activation energy.[130] This is similar to the situation in $LiFePO_4$.[133]

3.3. Other Compounds

Early studies in chalcogenide compounds showed that Na can also be intercalated in compounds such as TiS_2, TaS_2, $MoSe_2$, and $SnSe_yS_{2-y}$.[134–136] Na ions can occupy the inter-slab vacant sites in these materials. However, no extensive studies have been performed on these materials due to their poor electrochemical characteristics. Recently, Yamaki et al. suggested $NaMF_3$ as the positive electrode in NIB.[137–139] It was claimed that $NaMF_3$ can provide high safety as there is no risk of oxygen release during battery operation.[137] Various Na-free MF_3 (M = Fe, Ti, Co, Mn) compounds were electrochemically characterized.[138] Mössbauer spectroscopy before and after the discharge revealed that the $Fe^{2+/3+}$ redox couple was active in FeF_3-C electrodes giving a specific capacity of 150 mAh g^{-1} in NIB. Na-intercalated MF_3 compounds, $NaMF_3$ (M = Fe, Mn, Ni), was also directly synthesized via mechanochemical reaction and liquid-based synthesis.[137,139] Nanosized $NaFeF_3$ electrode could deliver 180 mAh g^{-1} at 1.5–4.5 V.

4. Challenges and Perspectives

Various classes of electrode materials for NIB were briefly introduced here. Overall, the performance of NIB still lags behind that of LIB at this moment. In a recent systematic first principles study comparing the properties of Li and Na intercalation compounds,[43,117] it was discussed that for anodes, the large ionic size of Na compared to Li can be disadvantageous in terms of volumetric energy density and cycling stability, in particular, for alloying compounds.[43] In addition, in the same crystal frameworks, Na compounds generally show a lower voltage compared to Li compounds as shown in **Figure 11** resulting in a reduction in energy density.[117] However, one interesting feature is that Na migration in layered frameworks ($ACoO_2$) can be more facile than Li migration. This is against the conventional belief

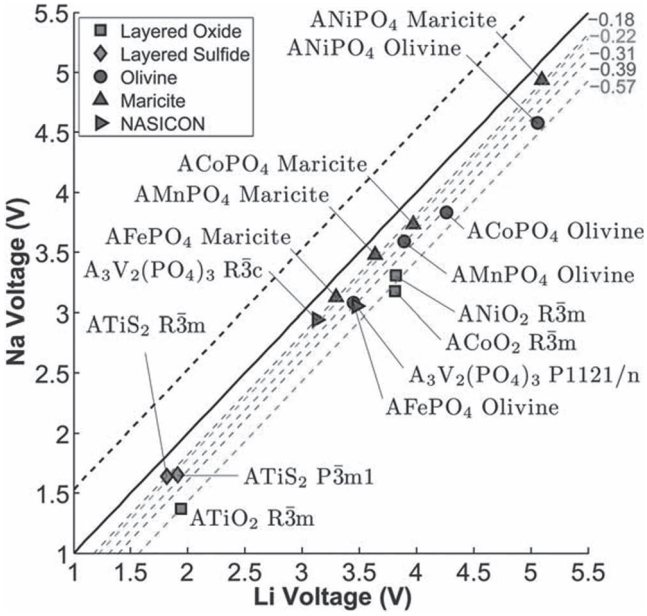

Figure 11. Calculated voltages of various compounds in vs. Na and vs. Li. Reproduced with permission.[117] Copyright 2011, Royal Society of Chemistry.

that Na diffuses slower in the identical host structures due to larger ionic size. Larger inter-slab distance in this structure was believed to reduce the diffusion barrier in $NaCoO_2$. This analysis does, however, not take into account the possible kinetic problems which may arise from gliding transitions between the oxygen layers, as discussed in this review.

Besides comparing the electrochemical performance of same crystal frameworks in LIB and NIB, there exist stable Na compounds whose Li analogues are not stable. For example, $NaFeF_3$ positive electrode is a new material whose Li analogue does not exist.[137,139]

Commonly, Na compounds and their Li analogues form similar crystal structures with small differences in lattice parameters, distortion, and local environment, but in some cases, they form completely different structures.[117,124,129] The difference in structural competition for Li and Na compounds does present opportunity for interesting new Na-intercalation materials. In the case of layered AMO_2 (M = V, Cr, Fe, Mn) materials, $NaMO_2$ shows good electrochemical activity whereas $LiMO_2$ has little or no capacity or loses its initial capacity rapidly.[15,18–21,24] A computational analysis of Li_xMnO_2 shows that Li in tetrahedral sites can stabilize Mn in tetrahedral sites, resulting a stable Li/Mn dumbbell configuration which serves as nucleus for the layered to spinel phase transformation.[140] In Na_xMnO_2, however, Na is unlikely to move to tetrahedral site and therefore can not stabilize Mn in a tetrahedral site, resulting better structural stability and hence better cyclability.[15] The above argument can possibly apply to V, Cr, Fe systems.

The comparison of layered Li_xMO_2 and Na_xMO_2 indicates that the effects of the difference in crystal structures on electrochemical properties should be case-by-case. Therefore, there may be superior NIB electrode materials which have not been discovered yet. About twice as many Na compounds than Li compounds are present in ICSD (inorganic crystallographic structure database). In addition, the examples in this review show that in many cases the Na-reaction behavior of a material is not trivially related to its behavior in a Li-cell. This implies that more potential candidates can be suggested for the NIB electrode materials, and that significant opportunity exists to explore high capacity Na electrode materials.

Acknowledgements

This research was supported by Energy Efficiency and Resources R&D program (20112020100070) under the Ministry of Knowledge Economy, Republic of Korea and by Human Resources Development of the Korea Institute of Energy Technology Evaluation and Planning (KETEP) grant funded by the Korea government Ministry of Knowledge Economy (20114010203120). This research was also supported by the Converging Research Center Program through the Ministry of Education, Science and Technology (2011K000691).

Received: January 10, 2012
Published online: May 14, 2012

[1] Y. Nishi, *J. Power Sources* **2001**, *100*, 101.
[2] S. Megahed, B. Scrosati, *J. Power Sources* **1994**, *51*, 79.
[3] K. Ozawa, *Solid State Ionics* **1994**, *69*, 212.
[4] J. M. Tarascon, M. Armand, *Nature* **2001**, *414*, 359.
[5] M. Armand, J. M. Tarascon, *Nature* **2008**, *451*, 652.
[6] B. Scrosati, *Electrochim. Acta* **2000**, *45*, 2461.
[7] M. R. Palacin, *Chem. Soc. Rev.* **2009**, *38*, 2565.
[8] B. Dunn, H. Kamath, J. M. Tarascon, *Science* **2011**, *334*, 928.
[9] WEBSITE: *http://www.nistep.go.jp/achiev/ftx/eng/stfc/stt039e/qr39pdf/STTqr3904.pdf*, accessed date: April, 2012.
[10] WEBSITE: *http://www.che.ncsu.edu/ILEET/phevs/lithium-availability/An_Abundance_of_Lithium.pdf,* accessed date: April, 2012.
[11] A. Shibata, K. Sato, *Power Eng. J.* **1999**, *13*, 130.
[12] D. Aurbach, Y. Gofer, Z. Lu, A. Schechter, O. Chusid, H. Gizbar, Y. Cohen, V. Ashkenazi, M. Moshkovich, R. Turgeman, E. Levi, *J. Power Sources* **2001**, *97–8*, 28.
[13] G. Girishkumar, B. McCloskey, A. C. Luntz, S. Swanson, W. Wilcke, *J. Phys. Chem. Lett.* **2010**, *1*, 2193.
[14] K. F. Blurton, A. F. Sammells, *J. Power Sources* **1979**, *4*, 263.
[15] X. Ma, H. Chen, G. Ceder, *J. Electrochem. Soc.* **2011**, *158*, A1307.
[16] B. L. Ellis, W. R. M. Makahnouk, Y. Makimura, K. Toghill, L. F. Nazar, *Nat. Mater.* **2007**, *6*, 749.
[17] A. R. Armstrong, P. G. Bruce, *Nature* **1996**, *381*, 499.
[18] S. Komaba, C. Takei, T. Nakayama, A. Ogata, N. Yabuuchi, *Electrochem. Commun.* **2010**, *12*, 355.
[19] C. Didier, M. Guignard, C. Denage, O. Szajwaj, S. Ito, I. Saadoune, J. Darriet, C. Delmas, *Electrochem. Solid-State Lett.* **2011**, *14*, A75.
[20] J. Li, J. Li, J. Luo, L. Wang, X. He, *Int. J. Electrochem. Sci.* **2011**, *6*, 1550.
[21] Y. Takeda, K. Nakahara, M. Nishijima, N. Imanishi, O. Yamamoto, M. Takano, R. Kanno, *Mater. Res. Bull.* **1994**, *29*, 659.
[22] L. Zhang, K. Takada, N. Ohta, M. Osada, T. Sasaki, *J. Power Sources* **2007**, *174*, 1007.
[23] D. A. Stevens, J. R. Dahn, *J. Electrochem. Soc.* **2001**, *148*, A803.
[24] D. P. Divincenzo, E. J. Mele, *Phys. Rev. B* **1985**, *32*, 2538.
[25] J. W. Jiang, J. R. Dahn, *Electrochim. Acta* **2004**, *49*, 4599.
[26] J. Sangster, *J. Phase Equilib. Diff.* **2007**, *28*, 571.
[27] P. Ge, M. Fouletier, *Solid State Ionics* **1988**, *28*, 1172.
[28] J. O. Besenhard, *Carbon* **1976**, *14*, 111.

[29] M. M. Doeff, Y. P. Ma, S. J. Visco, L. C. Dejonghe, *J. Electrochem. Soc.* **1993**, *140*, L169.
[30] P. Thomas, J. Ghanbaja, D. Billaud, *Electrochim. Acta* **1999**, *45*, 423.
[31] P. Thomas, D. Billaud, *Electrochim. Acta* **2001**, *46*, 3359.
[32] R. Alcantara, J. M. J. Mateos, J. L. Tirado, *J. Electrochem. Soc.* **2002**, *149*, A201.
[33] P. Thomas, D. Billaud, *Electrochim. Acta* **2002**, *47*, 3303.
[34] R. Alcantara, P. Lavela, G. F. Ortiz, J. L. Tirado, *Electrochem. Solid-State Lett.* **2005**, *8*, A222.
[35] X. Xia, M. N. Obrovac, J. R. Dahn, *Electrochem. Solid-State Lett.* **2011**, *14*, A130.
[36] D. A. Stevens, J. R. Dahn, *J. Electrochem. Soc.* **2000**, *147*, 1271.
[37] R. Alcantara, J. M. Jimenez-Mateos, P. Lavela, J. L. Tirado, *Electrochem. Commun.* **2001**, *3*, 639.
[38] S. Komaba, W. Murata, T. Ishikawa, N. Yabuuchi, T. Ozeki, T. Nakayama, A. Ogata, K. Gotoh, K. Fujiwara, *Adv. Funct. Mater.* **2011**, *21*, 3859.
[39] D. A. Stevens, J. R. Dahn, *J. Electrochem. Soc.* **2000**, *147*, 4428.
[40] J. Barker, R. K. B. Gover, P. Burns, A. J. Bryan, *Electrochem. Solid-State Lett.* **2006**, *9*, A190.
[41] S. Wenzel, T. Hara, J. Janek, P. Adelhelm, *Energy Environ. Sci.* **2011**, *4*, 3342.
[42] R. Alcantara, M. Jaraba, P. Lavela, J. L. Tirado, *Chem. Mater.* **2002**, *14*, 2847.
[43] V. L. Chevrier, G. Ceder, *J. Electrochem. Soc.* **2011**, *158*, A1011.
[44] D. Hamani, M. Ati, J. M. Tarascon, P. Rozier, *Electrochem. Commun.* **2011**, *13*, 938.
[45] S. Il Park, I. Gocheva, S. Okada, J. Yamaki, *J. Electrochem. Soc.* **2011**, *158*, A1067.
[46] P. Senguttuvan, G. Rousse, V. Seznec, J. M. Tarascon, M. R. Palacin, *Chem. Mater.* **2011**, *23*, 4109.
[47] Q. Sun, Q.-Q. Ren, H. Li, Z.-W. Fu, *Electrochem. Commun.* **2011**, *13*, 1462.
[48] S. Komaba, T. Mikumo, N. Yabuuchi, A. Ogata, H. Yoshida, Y. Yamada, *J. Electrochem. Soc.* **2010**, *157*, A60.
[49] A. Maazaz, C. Delmas, P. Hagenmuller, *J. Incl. Phenom. Macro. Chem.* **1983**, *1*, 45.
[50] S. I. Park, I. Gocheva, S. Okada, J. Yamaki, *J. Electrochem. Soc.* **2011**, *158*, A1067.
[51] P. Poizot, S. Laruelle, S. Grugeon, L. Dupont, J. M. Tarascon, *Nature* **2000**, *407*, 496.
[52] A. S. Arico, P. Bruce, B. Scrosati, J. M. Tarascon, W. Van Schalkwijk, *Nat. Mater.* **2005**, *4*, 366.
[53] A. V. Chadwick, S. L. P. Savin, S. Fiddy, R. Alcantara, D. F. Lisbona, P. Lavela, G. F. Ortiz, J. L. Tirado, *J. Phys. Chem. C* **2007**, *111*, 4636.
[54] T. B. Kim, J. W. Choi, H. S. Ryu, G. B. Cho, K. W. Kim, J. H. Ahn, K. K. Cho, H. J. Ahn, *J. Power Sources* **2007**, *174*, 1275.
[55] J. S. Kim, G. B. Cho, K. W. Kim, J. H. Ahn, G. Wang, H. J. Ahn, *Curr. Appl. Phys.* **2011**, *11*, S215.
[56] X. Liu, S. Kang, J. Kim, H. Ahn, S. Lim, I. Ahn, *Rare Metals* **2011**, *30*, 5.
[57] J. S. Kim, H. J. Ahn, H. S. Ryu, D. J. Kim, G. B. Cho, K. W. Kim, T. H. Nam, J. H. Ahn, *J. Power Sources* **2008**, *178*, 852.
[58] H. Kim, D.-H. Seo, S.-W. Kim, J. Kim, K. Kang, *Carbon* **2011**, *49*, 326.
[59] T. R. Jow, L. W. Shacklette, M. Maxfield, D. Vernick, *J. Electrochem. Soc.* **1987**, *134*, 1730.
[60] C. Delmas, J. J. Braconnier, C. Fouassier, P. Hagenmuller, *Solid State Ionics* **1981**, *3–4*, 165.
[61] J. J. Braconnier, C. Delmas, P. Hagenmuller, *Mater. Res. Bull.* **1982**, *17*, 993.
[62] F. Sauvage, L. Laffont, J. M. Tarascon, E. Baudrin, *Inorg. Chem.* **2007**, *46*, 3289.
[63] S. Komaba, T. Nakayama, A. Ogata, T. Shimizu, C. Takei, S. Takada, A. Hokura, I. Nakai, *ECS Trans.* **2009**, *16*, 43.
[64] C. Delmas, C. Fouassier, P. Hagenmuller, *Physica B&C* **1980**, *99*, 81.
[65] C. Fouassier, G. Matejka, J.-M. Reau, P. Hagenmuller, *J. Solid State Chem.* **1973**, *6*, 532.
[66] O. A. Smirnova, M. Avdeev, V. B. Nalbandyan, V. V. Kharton, F. M. B. Marques, *Mater. Res. Bull.* **2006**, *41*, 1056.
[67] A. R. Armstrong, M. Holzapfel, P. Novak, C. S. Johnson, S. H. Kang, M. M. Thackeray, P. G. Bruce, *J. Am. Chem. Soc.* **2006**, *128*, 8694.
[68] J. Reed, G. Ceder, *Chem. Rev.* **2004**, *104*, 4513.
[69] G. Ceder, A. Van der Ven, *Electrochim. Acta* **1999**, *45*, 131.
[70] R. Berthelot, D. Carlier, C. Delmas, *Nat. Mater.* **2011**, *10*, 74.
[71] A. Bhide, K. Hariharan, *Solid State Ionics* **2011**, *192*, 360.
[72] G. J. Shu, F. C. Chou, *Phys. Rev. B* **2008**, *78*.
[73] D. Carlier, J. H. Cheng, R. Berthelot, M. Guignard, M. Yoncheva, R. Stoyanova, B. J. Hwang, C. Delmas, *Dalton Trans.* **2011**, *40*, 9306.
[74] A. Caballero, L. Hernan, J. Morales, L. Sanchez, J. S. Pena, M. A. G. Aranda, *J. Mater. Chem.* **2002**, *12*, 1142.
[75] Z. H. Lu, J. R. Dahn, *J. Electrochem. Soc.* **2001**, *148*, A1225.
[76] S. Miyazaki, S. Kikkawa, M. Koizumi, *Synthetic Met.* **1983**, *6*, 211.
[77] Y. Makimura, T. Ohzuku, *J. Power Sources* **2003**, *119–121*, 156.
[78] N. Yabuuchi, Y.-C. Lu, A. N. Mansour, S. Chen, Y. Shao-Horn, *J. Electrochem. Soc.* **2011**, *158*, A192.
[79] K. S. Kang, Y. S. Meng, J. Breger, C. P. Grey, G. Ceder, *Science* **2006**, *311*, 977.
[80] D. Kim, S. H. Kang, M. Slater, S. Rood, J. T. Vaughey, N. Karan, M. Balasubramanian, C. S. Johnson, *Adv. Energy Mater.* **2011**, *1*, 333.
[81] J. Hong, D. H. Seo, S. W. Kim, H. Gwon, S. T. Oh, K. Kang, *J. Mater. Chem.* **2010**, *20*, 10179.
[82] C. P. Grey, W. S. Yoon, J. Reed, G. Ceder, *Electrochem. Solid-State Lett.* **2004**, *7*, A290.
[83] Z. H. Lu, J. R. Dahn, *J. Electrochem. Soc.* **2002**, *149*, A815.
[84] J. Reed, G. Ceder, *Electrochem. Solid-State Lett.* **2002**, *5*, A145.
[85] W. F. Wei, X. W. Cui, W. X. Chen, D. G. Ivey, *Chem. Soc. Rev.* **2011**, *40*, 1697.
[86] J. M. Tarascon, D. G. Guyomard, B. Wilkens, W. R. McKinnon, P. Barboux, *Solid State Ionics* **1992**, *57*, 113.
[87] S. Bach, M. Millet, J. P. Periera-Ramos, L. Sanchez, P. Lavela, J. L. Tirado, *Electrochem. Solid-State Lett.* **1999**, *2*, 545.
[88] M. M. Doeff, M. Y. Peng, Y. P. Ma, L. C. Dejonghe, *J. Electrochem. Soc.* **1994**, *141*, L145.
[89] J. A. Saint, M. M. Doeff, J. Wilcox, *Chem. Mater.* **2008**, *20*, 3404.
[90] Y. L. Cao, L. F. Xiao, W. Wang, D. W. Choi, Z. M. Nie, J. G. Yu, L. V. Saraf, Z. G. Yang, J. Liu, *Adv. Mater.* **2011**, *23*, 3155.
[91] A. D. Tevar, J. F. Whitacre, *J. Electrochem. Soc.* **2010**, *157*, A870.
[92] Y. Shao-Horn, S. A. Hackney, A. R. Armstrong, P. G. Bruce, R. Gitzendanner, C. S. Johnson, M. M. Thackeray, *J. Electrochem. Soc.* **1999**, *146*, 2404.
[93] K. West, B. Zachauchristiansen, T. Jacobsen, S. Skaarup, *Solid State Ionics* **1988**, *28*, 1128.
[94] S. Bach, N. Baffier, J. P. Pereiraramos, R. Messina, *Solid State Ionics* **1989**, *37*, 41.
[95] J. P. Pereiraramos, R. Messina, S. Bach, N. Baffier, *Solid State Ionics* **1990**, *40–1*, 970.
[96] H. M. Liu, H. S. Zhou, L. P. Chen, Z. F. Tang, W. S. Yang, *J. Power Sources* **2011**, *196*, 814.
[97] Z. L. Gong, Y. Yang, *Energy Environ. Sci.* **2011**, *4*, 3223.
[98] A. K. Padhi, K. S. Nanjundaswamy, J. B. Goodenough, *J. Electrochem. Soc.* **1997**, *144*, 1188.
[99] S. P. Ong, A. Jain, G. Hautier, B. Kang, G. Ceder, *Electrochem. Commun.* **2010**, *12*, 427.
[100] S. W. Kim, J. Kim, H. Gwon, K. Kang, *J. Electrochem. Soc.* **2009**, *156*, A635.

[101] G. Hautier, A. Jain, S. P. Ong, B. Kang, C. Moore, R. Doe, G. Ceder, *Chem. Mater.* **2011**, *23*, 3495.
[102] C. Delmas, A. Nadiri, J. L. Soubeyroux, *Solid State Ionics* **1988**, *28*, 419.
[103] J. B. Goodenough, H. Y. P. Hong, J. A. Kafalas, *Mater. Res. Bull.* **1976**, *11*, 203.
[104] C. Delmas, F. Cherkaoui, A. Nadiri, P. Hagenmuller, *Mater. Res. Bull.* **1987**, *22*, 631.
[105] A. K. Padhi, K. S. Nanjundaswamy, C. Masquelier, J. B. Goodenough, *J. Electrochem. Soc.* **1997**, *144*, 2581.
[106] K. S. Nanjundaswamy, A. K. Padhi, J. B. Goodenough, S. Okada, H. Ohtsuka, H. Arai, J. Yamaki, *Solid State Ionics* **1996**, *92*, 1.
[107] G. X. Wang, D. H. Bradhurst, S. X. Dou, H. K. Liu, *J. Power Sources* **2003**, *124*, 231.
[108] L. S. Plashnitsa, E. Kobayashi, Y. Noguchi, S. Okada, J. Yamaki, *J. Electrochem. Soc.* **2010**, *157*, A536.
[109] J. Barker, M. Y. Saidi, J. L. Swoyer, *Electrochem. Solid-State Lett.* **2003**, *6*, A1.
[110] R. K. B. Gover, A. Bryan, P. Burns, J. Barker, *Solid State Ionics* **2006**, *177*, 1495.
[111] F. Sauvage, E. Quarez, J. M. Tarascon, E. Baudrin, *Solid State Sciences* **2006**, *8*, 1215.
[112] C. Delacourt, L. Laffont, R. Bouchet, C. Wurm, J. B. Leriche, M. Morcrette, J. M. Tarascon, C. Masquelier, *J. Electrochem. Soc.* **2005**, *152*, A913.
[113] S. Okada, S. Sawa, M. Egashira, J. Yamaki, M. Tabuchi, H. Kageyama, T. Konishi, A. Yoshino, *J. Power Sources* **2001**, *97–8*, 430.
[114] A. K. Padhi, K. S. Nanjundaswamy, C. Masquelier, S. Okada, J. B. Goodenough, *J. Electrochem. Soc.* **1997**, *144*, 1609.
[115] C. M. Burba, R. Frech, *Spectrochim. Acta A* **2006**, *65*, 44.
[116] P. Moreau, D. Guyomard, J. Gaubicher, F. Boucher, *Chem. Mater.* **2010**, *22*, 4126.
[117] S. P. Ong, V. L. Chevrier, G. Hautier, A. Jain, C. Moore, S. Kim, X. H. Ma, G. Ceder, *Energy Environ. Sci.* **2011**, *4*, 3680.
[118] K. T. Lee, T. N. Ramesh, F. Nan, G. Botton, L. F. Nazar, *Chem. Mater.* **2011**, *23*, 3593.
[119] C. Delacourt, P. Poizot, J. M. Tarascon, C. Masquelier, *Nat. Mater.* **2005**, *4*, 254.
[120] D.-H. Seo, H.Gwon, S.-W. Kim, J. Kim, K. Kang, *Chem. Mater.* **2010**, *22*, 518.
[121] Park, R. A. Shakoor, K.-Y. Park, K. Kang, *J. Electrochem. Sci. Tech.*, **2011**, *2*, 14.
[122] T. Shiratsuchi, S. Okada, J. Yamaki, T. Nishida, *J. Power Sources* **2006**, *159*, 268.
[123] P. Barpanda, J. N. Chotard, N. Recham, C. Delacourt, M. Ati, L. Dupont, M. Armand, J. M. Tarascon, *Inorg. Chem.* **2010**, *49*, 7401.
[124] B. L. Ellis, W. R. M. Makahnouk, W. N. Rowan-Weetaluktuk, D. H. Ryan, L. F. Nazar, *Chem. Mater.* **2010**, *22*, 1059.
[125] R. Tripathi, T. N. Ramesh, B. L. Ellis, L. F. Nazar, *Angew. Chem. Int. Ed.* **2010**, *49*, 8738.
[126] Y. Kawabe, N. Yabuuchi, M. Kajiyama, N. Fukuhara, T. Inamasu, R. Okuyama, I. Nakai, S. Komaba, *Electrochem. Commun.* **2011**, *13*, 1225.
[127] I. K. Lee, I. B. Shim, C. S. Kim, *J. Appl. Phys.* **2011**, *109*, 07E136.
[128] M. Reynaud, P. Barpanda, G. Rousse, J.-N. Chotard, B. C. Melot, N. Recham, J.-M. Tarascon, *Solid State Sci.* **2011**, *14*, 15.
[129] R. Tripathi, G. R. Gardiner, M. S. Islam, L. F. Nazar, *Chem. Mater.* **2011**, *23*, 2278.
[130] T. Mueller, G. Hautier, A. Jain, G. Ceder, *Chem. Mater.* **2011**, *23*, 3854.
[131] N. Recham, J. N. Chotard, L. Dupont, K. Djellab, M. Armand, J. M. Tarascon, *J. Electrochem. Soc.* **2009**, *156*, A993.
[132] X. Wu, J. Zheng, Z. Gong, Y. Yang, *J. Mater. Chem.* **2011**, *21*, 18630.
[133] R. Malik, D. Burch, M. Bazant, G. Ceder, *Nano Lett.* **2010**, *10*, 4123.
[134] A. S. Nagelberg, W. L. Worrell, *J. Solid State Chem.* **1979**, *29*, 345.
[135] J. Morales, J. Santos, J. L. Tirado, *Solid State Ionics* **1996**, *83*, 57.
[136] J. Morales, C. P. Vicente, J. Santos, J. L. Tirado, *Electrochim. Acta* **1997**, *42*, 357.
[137] I. D. Gocheva, M. Nishijima, T. Doi, S. Okada, J. Yamaki, T. Nishida, *J. Power Sources* **2009**, *187*, 247.
[138] M. Nishijima, I. D. Gocheva, S. Okada, T. Doi, J. Yamaki, T. Nishida, *J. Power Sources* **2009**, *190*, 558.
[139] Y. Yamada, T. Doi, I. Tanaka, S. Okada, J.-i. Yamaki, *J. Power Sources* **2011**, *196*, 4837.
[140] J. Reed, G. Ceder, A. Van Der Ven, *Electrochem. Solid-State Lett.* **2001**, *4*, A78.
[141] Z. Jian, L. Zhao, H. Pan, Y.-S. Hu, H. Li, W. Chen, L. Chen, *Electrochem. Commun.* **2011**, *14*, 86.